



## A Smart Rig for Calibration of Gas Sensor Nodes: Test and Deployment

---

Abderrazak Abdaoui, Farid Touati, Hasan Tariq and  
Adel Ben Mnouar

EasyChair preprints are intended for rapid dissemination of research results and are integrated with the rest of EasyChair.

June 14, 2020

# A Smart Rig for Calibration of Gas Sensor Nodes: Test and Deployment

1<sup>st</sup> Abderrazak Abdaoui    2<sup>nd</sup> Farid Touati    3<sup>rd</sup> Hasan Tariq  
email: {abderrazak.abdaoui, touatif, hasan.tariq}@qu.edu.qa  
Electrical Engineering Department College of Engineering,  
Qatar University, Doha, Qatar,

4<sup>th</sup> Adel Ben Mnouar  
e-mail: adel@tud.ac.ae  
Canadian University Dubai,  
United Arab Emirates (UAE)

**Abstract**—Nowadays, large number of sensors are deployed and used for air quality monitoring or in some industries that process hazardous gases. These sensors need periodic calibration to ensure reliable measurements. This paper proposes a dedicated smart calibration rig with a set of novel features enabling complete automation and parallel or batch calibration. The calibration process is completely automated by developing a LabVIEW-based platform that controls the calibration environment for the sensor nodes under test by logging sensor data, generates an updated calibration equation and uploading it to the sensor node for next deployments. The results demonstrate the effectiveness of the sensor calibration rig.

**Index Terms**—Gas sensors calibration, cross-sensitivity, piecewise curve fitting, IEEE 802.15.4, ZigBee.

## I. INTRODUCTION

In our life, with the degradation of the air quality, in indoor and outdoor environments, gas sensors are actively employed to monitor the quality of air and increase the human safety. Some types of these sensors are used for monitoring and controlling the combustion processes [1]–[3]. Oxygen and other types of sensors are used in medical applications, for example for analyzing human breath [4], [5].

The air quality, are strongly important to comfort levels and human health. In recent years, indoor air quality has received more attention and research than outdoor air quality, since (i) the concentration of some pollutants is two to five times higher indoor than outdoor, and (ii) people and in particular elderly spend up to 90% of their time indoors [6]. Air quality has been traditionally monitored using networks of routine measuring static stations often supplemented by modeling [7]–[9]. These stations are usually reliable and can accurately measure a wide range of air pollutants. However, most gas sensors, suffer from long term drift and aging problems. Calibration of such devices is usually required to guarantee reliability of measurements.

The process of gas sensor calibration is tedious and includes (i) collection of sensor response at different operating points, (ii) data processing and determination of appropriate mathematical model linking the real gas concentration to the sensor response, and (iii) storing of the calibration model or look-up tables in a memory associated with the sensor to correct its readings during subsequent deployments.

This paper presents an automated calibration rig for the simultaneous calibration of multiple sensors; the calibration steps are pre-programmed and the operator intervention is

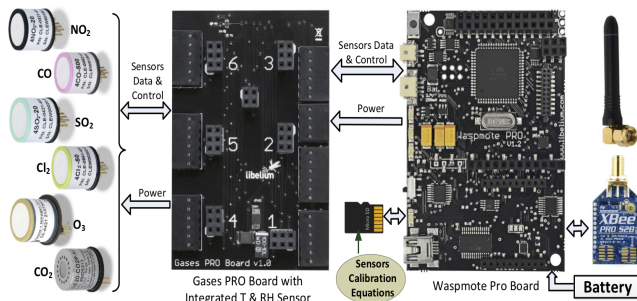


Fig. 1. Indoor Air Quality sensor node.

minimal. We employ LabVIEW to monitor the calibration and data measurements for the calibration Rig. This LabVIEW controller rig enables simultaneous testing of several wireless sensor nodes that include sensors for multiple target gases. Suitable mathematical algorithm, based on piecewise approximation, is developed for the calibration of each sensor under test. To the best knowledge of the authors, this approach of automatic calibration of sensor nodes has not been reported before. The remainder of the paper is organized as follows. Section II presents the sensor nodes used in the present work. Section III describes the hardware and software operation details of the calibration rig. Section IV presents results with further discussions. The paper is concluded in Section V.

## II. AIR QUALITY (IAQ) SENSING NODE

The proposed automated rig may be used to calibrate any gas sensors or gas sensor nodes. However, the presented calibration method is applied to wireless sensor nodes used for measurement of indoor and outdoor air quality, and described in [10].

The air quality sensing node has been designed using sensors from Libelium. Based on their principle of operation there are two groups of gas sensors used in the node; electrochemical sensors for CO, Cl<sub>2</sub>, O<sub>3</sub>, NO<sub>2</sub> and SO<sub>2</sub> and non-dispersive infrared (NDIR) CO<sub>2</sub> sensors. Each sensor is equipped with an Analog Front End (AFE) interface that includes the electronics that run the sensor and an EEPROM in which sensor-related information (e.g. sensor type, gas type, measurement range) and factory calibration data are stored. The AFE for each amperometric sensor (other

than CO<sub>2</sub>) includes a trans-impedance amplifier that converts the sensor current into voltage. Note that the sensors are factory-calibrated and that the calibration data is stored in the EEPROM of the AFE; however, sensor re-calibration by the user cannot be performed by using the EEPROM. Hence, the calibration method described below is based on the update of memories integrated into the processor board of the sensor node.

The key components of the sensor node hardware are illustrated in Fig. I. Each node incorporates two boards: a board on which sensors are plugged (left side) and a processor board (right side). The latter board includes mainly a micro-controller, a data transfer wireless module (Xbee PRO), and a micro SD card. The micro-controller performs signal processing on the sensor data and controls the flow of data between the node and the outside world through the Xbee PRO module.

### III. CALIBRATION RIG DESIGN

The hardware of the automated PC based test rig is composed of a gas blending system and a temperature control system. Identical sensors are calibrated together under same conditions for consistency and accuracy. The calibration data, for each sensor, is used to generate piecewise functions (using a mathematical algorithm) whose coefficients are stored locally in the PC under associated unique ID. Prior to field deployment, the piecewise function coefficients are wirelessly uploaded to each sensor in the node. The sensor node stores the calibration data in the micro SD card for further air quality monitoring. For recalibration, the sensor nodes are retreated from the field and placed in the rig where the existing calibration data gets overwritten with latest calibration results.

#### A. Calibration rig Hardware

##### *Gas mixing system*

The proposed setup for the calibration rig includes an array of gas cylinders, a gas blending system that provides continuous variation of mixture composition, sealed chamber with temperature control, and a process control PC unit. The gas blending is performed using mass-flow controllers (MFCs). The composition of the test gas mixture resulting from blending, that is inlet to the sealed chamber, is adjusted by controlling the MFCs using the control PC through flow of individual gas components. The MFCs have the standard RS485 communication interfaces to exchange data with the PC that runs the rig. The outlet of the chamber is connected to a bubbler to seal the system and expel test gases safely into the atmosphere through appropriate piping. One of the gas cylinders contains pure air and the other contains pre-mixed target gases (diluted in air, with fixed concentration  $g_X^c$  in ppm). To set the concentration  $g_X$  of the target gas X in the sealed environmental chamber, the flow rates  $f_X$  and  $f_{AIR}$  of premixed target gas and air, respectively, are adjusted by  $MFC_X$  and of  $MFC_{AIR}$  according to (1),

$$f_X = \frac{g_X}{g_X^c} (f_X + f_{AIR}) \quad (1)$$

Evidently, the dilution of the target gas requires mixing it with at least another gas, for example air in which case  $f_{total} = f_X + f_{AIR}$ . Hence, either the flow of pure air ( $f_{AIR}$ ) is fixed first and the flow of the diluted gas ( $f_X$ ) is determined, or the total flow ( $f_X + f_{AIR}$ ) is fixed and both  $f_X$  and  $f_{AIR}$  are determined.

#### B. Computer and software tools

LabVIEW platform has been used to develop the software that controls the entire calibration process. Through the developed software, the process control pc achieves the two main following tasks:

- Control the composition of the gas and temperature inside the chamber.
- Calibration processing and storing the calibration data in the sensor node under test.

First, based on the test requirements, the software programs the MFC flow rates serially over RS485 communication link to control the desired gas composition in the chamber. For each test point, the software reads and stores the sensor data locally. Second, the calibration of sensor nodes is accomplished in two steps:

- 1) Testing the node at various concentrations of each target gas, collecting the data and generating a calibration equation for each sensor.
- 2) Uploading the calibration equations into the SD card of the sensor node.

There are two possible ways of testing the node sensors:

- 1) Sensors of the same type are mounted on the same node and calibrated together. Calibrating identical sensors together provides two-fold benefits: it reduces the volume of gas required for calibrating sensors, and it ensures that all sensors have been calibrated for the same test points under same conditions.
- 2) Multiple sensor nodes, with their associated various sensors, may be tested together. This approach enables direct assessment of sensors cross-sensitivity as the response of each sensor is due to its exposure, thus its sensitivity, to all the gases being flown into the chamber and not only to the associated gas.

A dedicated application protocol based on master-slave communication structure has been designed, where the process control PC acts as the master and the sensor node as the slave. The protocol has been designed considering speed and reliability of communication taking into account the simplicity of implementation. The messages are composed using bytes over strings for conciseness to improve the speed of communication.

1) *Collection of sensors measurement data*:: During data collection phase, sensor/sensor nodes are placed inside the environmental chamber of the calibration rig. During this process, the sensor node should be programmed to operate in the measurement mode. Through the sensor node firmware, when the measurement mode is selected, the (voltage/current) data, collected from the sensors, are directly transmitted through

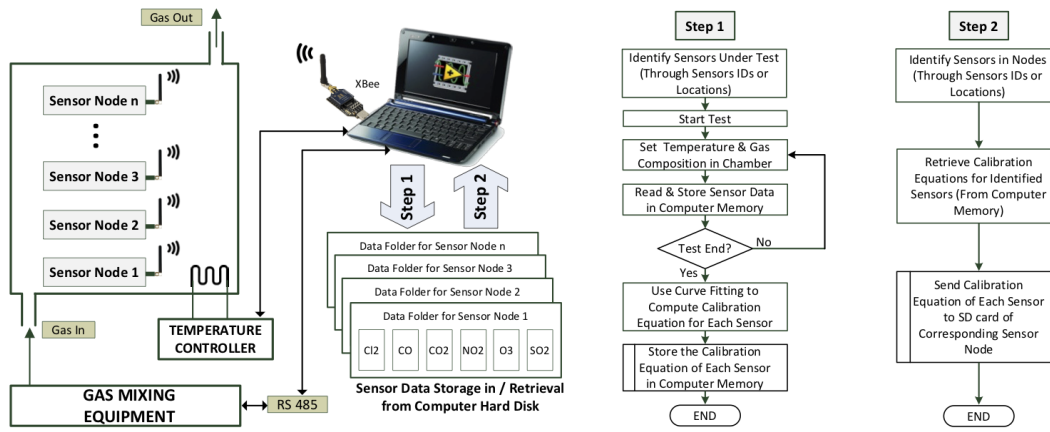


Fig. 2. LabVIEW VI running the calibration rig during data collection phase.

ZigBee to the LabVIEW PC. However, after calibration and updating the SD card by the polynomial coefficients, the measurements collected from the sensors are converted to physical values by applying the associated polynomial function identified by the sensor serial number. As discussed above, the computer-MFCs are used to set specific target gas concentrations inside the chamber by mixing streams of target gases with pure air according to (1). It is therefore critical to assess the time needed to wait before the gas concentration in the chamber settles down following a computer command to change the flow rates of the MFCs.

Following the time response test above, the wait time can be determined for each sensor for various concentrations of the relevant target gas. For calibration purposes, the range of concentration of a given target gas X is determined according to the expected range in indoor air. Nevertheless, a minimum number of test points within this range is also needed to ensure that any non-linearity of sensor response within the calibration range will be recorded. As described previously, the rig allows simultaneous testing of multiple sensors/sensor nodes. The LabVIEW software starts by identifying the IDs (stored in the EEPROM of the AFE of the sensor) of all sensors placed in the environmental chamber of the test rig. These IDs include the type X of target gas, which will be used to sort out the various types of sensors for subsequent tests. A file is created for each sensor; the file name includes the sensor ID (including the absolute serial number) for easy identification. Also, the identification of the sensor type leads to knowledge of the corresponding target gas; pre-stored set point concentrations are stored in the LabVIEW VI for each target gas X. The sensors may be tested at real-world operating temperatures. The temperature may be set in the environmental chamber using the temperature controller. However, since the deployment is for indoor air quality monitoring, temperature is not expected to vary significantly as indoor temperature is usually adjusted for thermal comfort of people in these indoor environments. If, however, temperature is expected to vary significantly to a point it does affect sensors outputs, the rig allows finding the correlation of sensors outputs with ambient

temperature for ultimate temperature compensation of these sensors outputs. The data collection for each set of sensors, with target gas X, starts by setting the first concentration of target gas (from the pre-stored set points) through control of the corresponding MFCs according to equation (1). Then the program waits for the pre-stored wait time before reading the outputs of the set of sensors for target gas X. Averaging for multiple readings for each setpoint ensures minimization of the effects of noise. The set point concentration (SPC) and the corresponding sensor output are then stored in the corresponding sensor file.

In the present work, we employed the specific LabVIEW virtual instrument (VI) for curve fitting. The graphical user interface (GUI) of the curve fitting algorithm is used to read the measurement file of a set of sensors already generated during the first step of the calibration. Fig. 3 illustrates the GUI of the curve fitting where we can see two main parts: calibration input and calibration results. In the calibration input, we just personalize the location of the file containing the one calibration scene, the order of the polynomial and the  $R^2$  value. The LabVIEW module reads the file and automatically extracts the id (absolute serial number) of all the gas sensors registered in the data file. With the set of couple (set point concentration, voltage measurements) averaged on 5 values, the polynomial coefficients are produced for each sensor node and the results are displayed in the Calibration results part. The polynomial coefficients are then stored in a text form of the following form :

```

Calibrationfile - Notepad
File Edit Format View Help
Calibration <--polynomial coefficients-->
Serial      Timestamp  an  a1  a0  R squared
-----
CO-CLEW01278-T2  20180715125309  -0.016917  1.920001  24.529729  R2=0.997552
CO-CLEW01265-T2  20180715125319  -0.023336  2.312551  21.173297  R2=0.997201
CO-CLEW01225-T2  20180715125329  -0.022222  2.246836  21.780244  R2=0.997573
CO-CLEW01257-T2  20180715125343  -0.030183  2.409039  30.304216  R2=0.997416
CO-CLEW01271-T2  20180715125352  -194.12738  -1226.440958  -1854.394846  R2=0.633470
CO-CLEW01263-T2  20180715125406  -0.024742  2.357655  22.372482  R2=0.997333
CO2-IRMS7835  2018071511129  -0.010927  18.972183  -5837.892604  R2=0.993695
CO2-IRMS7822  20180715134253  6.587963E-5  -0.119117  76.517012  -15574.309949  R2=0.996143
CO2-IRM41928  20180715140304  1.832795E-5  -0.046952  43.757462  -12527.851541  R2=0.997149

```

A short description of each parameter is given below. This

polynomial fit operates by putting the arrays of X and Y values (sensor readings and set point concentrations, respectively). The Coefficient Constraint specifies the constraints on Polynomial Coefficients of certain orders by setting the coefficient of order to the coefficient option. Nonetheless, the order may specify the constrained polynomial order. The Polynomial Order (PO) specifies the desired order of the polynomial that is intended for data fitting. The PO can be set to any number between 1 and 25; the default order is 2. The Weight is the array of weights for the observations (X, Y). If the Weight is left disconnected as in the present application, the polynomial fit sets all elements of Weight to a default of 1. The method specifies the fitting method used: Least Square (default, used in the present application), Least Absolute Residual, or Bisquare.

The tolerance input (not used in the present application) determines when to stop the iterative adjustment of Polynomial Coefficients when either the Least Absolute Residual or the Bisquare method is used. For the Least Absolute Residual method, if the relative difference between residue in two successive iterations is less than the tolerance, this polynomial fit returns the resulting Polynomial Coefficients. For the Bisquare method, if any relative difference between Polynomial Coefficients in two successive iterations is less than the tolerance, this VI returns the resulting Polynomial Coefficients. The Algorithm input specifies the algorithm the VI uses to compute the next Polynomial Fit; the default is the singular value decomposition (SVD) algorithm (used in the present application).

The best Polynomial Fit output returns the Y-values ( $f_i$ ) of the polynomial curve that best fit the input values ( $y_i$ ). The Polynomial Coefficients output returns the coefficients of the fitted model in ascending order of power. The total number of elements in Polynomial Coefficients is PO + 1, where PO is the polynomial order. The Residue output returns the weighted mean error of the fitted model. When the Least Square method is used (as is in our case), the VI finds the Polynomial Coefficients of the polynomial model by minimizing the residue according to the following equation:

$$VAR_{res} = \frac{1}{N} \sum_{i=1}^N w_i (y_i - f_i) \quad (2)$$

where  $N$  is the length of array  $Y = \{y_1, \dots, y_N\}$ ,  $y_i$  is the  $i$ th element of  $Y$ ,  $w_i$  is the weight of the  $i$ th element,  $f_i$  is the  $i$ th element of Best Polynomial Fit. In our case, and in most-widely used applications, the weights of all elements are equal and therefore  $w_i = 1$ . As it is shown further down, in the present application, the residue is used to determine the  $R^2$  (calculated outside the polynomial fit). The latter is used to decide on the appropriate order of Polynomial Order to choose.

The experimental data is assumed to have been collected during step 1. The coefficients of the polynomial together with the goodness of fit parameter(s) are provided by the General Polynomial Fit VI. There are various parameters that may be used to evaluate how good is the fitting curve to the data. Since

the least square method is used for implementing the fitting algorithm, in the General Polynomial Fit VI, the optimization of the polynomial coefficients is done by minimizing the residue that represents the variance given in (2). This optimization assumes that the PO is already set. This residue ( $VAR_{res}$ ) and the variance output of the Standard Deviation and Variance VI are used to determine  $R^2$  of the best fit.

$$R^2 = 1 - \frac{VAR_{res}}{VAR_{tot}} \quad (3)$$

$R^2$  is then used to assess whether the resulting PO is acceptable. If  $R^2$  is below a pre-determined target, then the PO is incremented and the General Polynomial Fit VI is run again to find new polynomial coefficients and associated residue. The process is repeated until the value of  $R^2$  reaches the pre-determined target or the PO reaches its highest permitted value. Therefore the maximum PO depends on the number of test points used for a given sensor. At the end of the curve fitting process, the time-stamped polynomial coefficients and  $R^2$  value are stored in the sensor calibration file in the process control PC hard disk where the file is identified by the unique sensor ID.

2) *Sensor Calibration*: The polynomial fitting, applied to the data collected from each sensor, results in finding the polynomial coefficients that are used for the calibration of the sensor. The process of uploading the sensor-specific polynomial coefficients to the sensor node is strait-forward. During this process, the sensors to be calibrated are placed in their respective nodes which should be programmed to operate in the calibration mode. The calibration process starts by reading the IDs of the sensors of the nodes and then, after checking, stores the calibration data the relative sensor on the board. During monitoring mode, the ID of each sensor present on the Gas sensor board is then used to identify the corresponding line stored in SD card of the sensor board. Each measured voltage (in mV) indicating the gas concentration, is converted to calibrated concentration (ppm) by applying the polynomial function of the identified sensor.

#### IV. RESULTS

In this section, we present the implementation of the three calibration steps detailed in the previous sections for CO sensor and example of deployment of sensor boards in sub-urban environments.

##### A. Calibration of gas sensor : example of Carbon Monoxide (CO)

For the calibration, we first collect the measurement data for each sensor separately. Then, based on the set point gas concentrations and on the measured gas concentrations for each sensor node, we use LabVIEW to generate the polynomial fitting coefficients. Finally, we update the calibration file on the SD card for each sensor. At least one additional set of measurements is carried out to verify the results (see Fig. 4 and 5 below). We found that the waiting time depends on the gas flow rate used in the experiments, on the volume

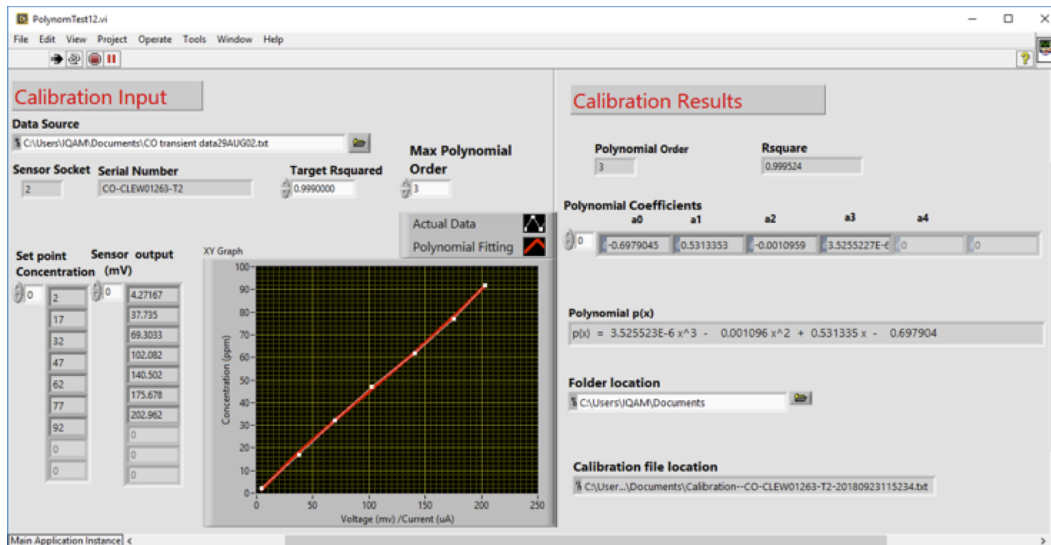
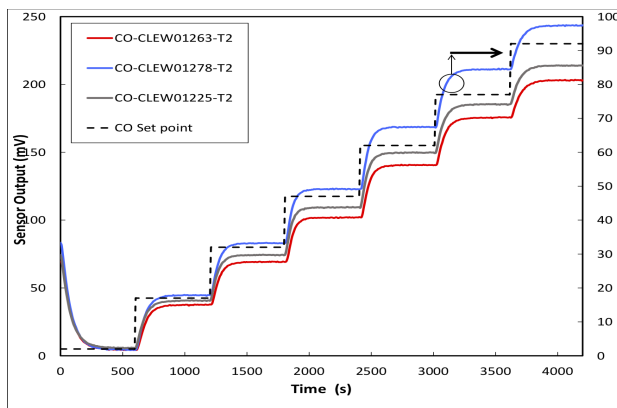
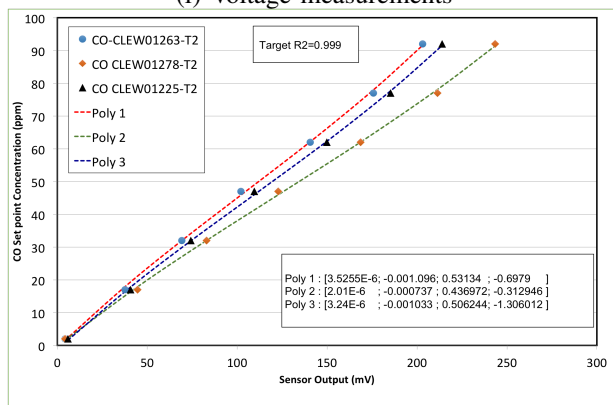


Fig. 3. Graphical User Interface for the LabVIEW VI for the polynomial fitting.



(i) Voltage measurements



(ii) Polynoms fitting

Fig. 4. CO sensor response to stepping of CO concentration.

of the tubing, on the environmental chamber, on the number of sensor nodes inside the chamber, and evidently on the response time of sensors. Fig. 4(i) shows the response time of three CO sensors before calibration that were exposed to

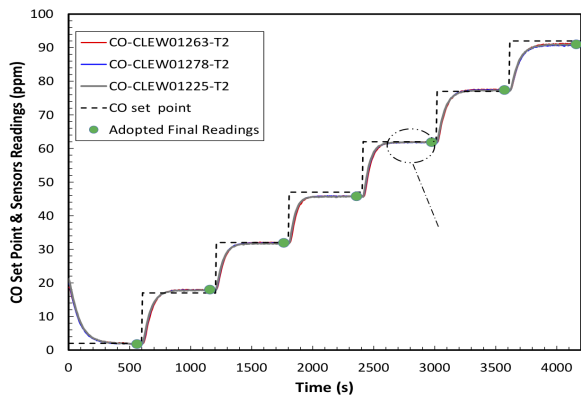
the same CO concentration stepping. Although, the estimated sensor wait time is approximately 3 minutes for all sensors, the response voltage level is different, which translates into different (wrong) CO concentration readings as shown in Fig. 4(ii). Obviously, the output is different for all sensors. However, for consistency, the outputs must be the same under same gas condition and hence the sensors should be calibrated. Fig. 5(i) depicts the results we obtained after calibrating the same previous three CO sensors. The coefficients of the best polynomials that were obtained during the calibration process are shown on the inset Fig. 5(ii). The data collection used for calibration was done at room temperature ( $22^{\circ}\text{C}$ ), and the target  $R^2$  was set to 0.999. Recall that the target  $R^2$  represents the required minimum value for  $R^2$  of the polynomials, and therefore the target  $R^2$  was used to select the order of the polynomial.

### B. Real Deployment of Gas Sensors

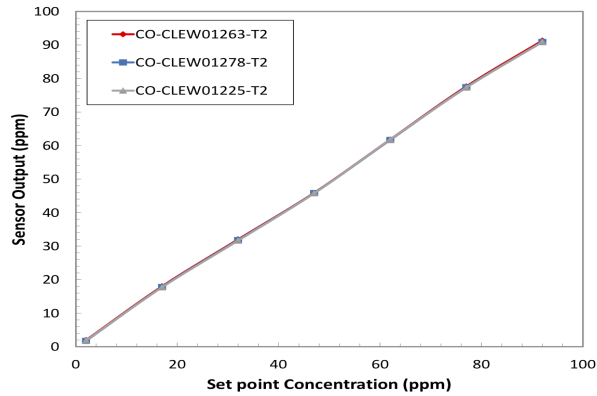
In this part, we evaluate the deployment of the sensor boards for long duration using solar panel (6 watts, 5 Volts) for energy harvesting. Figures 6, illustrates the sensor measurements from the Libellium boards from outdoor environments at QU and in the urban city (Mansoura) in Doha.

## V. CONCLUSION

In this paper, we presented a new practical calibration system that is dedicated to gas sensors for outdoor and indoor air quality monitoring. We proposed a complete calibration framework with a set of novel features. The calibration rig has been completely automated by developing a LabVIEW-based platform that controls the whole process such as control of calibration phases, data communication and collection, and flow rate of each mass flow control. The results demonstrated the effectiveness of the sensor calibration rig and the accuracy of the measurements of each calibrated sensor. Also, the measured data stored by the sensor nodes during calibration



(i) Voltage measurements



(ii) Polynoms fitting

Fig. 5. CO sensor response to stepping of CO concentration.

are essential for further data mining and development of more effective calibration models. In future work, we will focus our efforts to extend the use of this calibration rig platform for a large variety of sensors and sensor boards.

#### ACKNOWLEDGMENT

This publication was made possible by the National Priority Research Program (NPRP) award [NPRP10-0102-170094] from the Qatar National Research Fund (QNRF); a member of the Qatar Foundation.

#### REFERENCES

- [1] I. I. Soykal, P. H. Matter, L. B. Thrun, R. Q. Long, S. L. Swartz, and U. S. Ozkan, "Amperometric NO<sub>x</sub> sensor based on oxygen reduction," *IEEE Sensors Journal*, vol. 16, no. 6, pp. 1532–1540, 2015.
- [2] M. Benammar, "Techniques for measurement of oxygen and air-to-fuel ratio using zirconia sensors. a review," *Measurement Science and Technology*, vol. 5, no. 7, p. 757, 1994.
- [3] B. Ojha, N. Illyaskuty, J. Knoblauch, M. R. Balachandran, and H. Kohler, "High-temperature CO/HC gas sensors to optimize firewood combustion in low-power fireplaces," *Journal of Sensors and Sensor Systems*, vol. 6, no. 1, p. 237, 2017.
- [4] A. D. Wilson, "Advances in electronic-nose technologies for the detection of volatile biomarker metabolites in the human breath," *Metabolites*, vol. 5, no. 1, pp. 140–163, 2015.
- [5] C. Di Natale, R. Paolesse, E. Martinelli, and R. Capuano, "Solid-state gas sensors for breath analysis: A review," *Analytica chimica acta*, vol. 824, pp. 1–17, 2014.

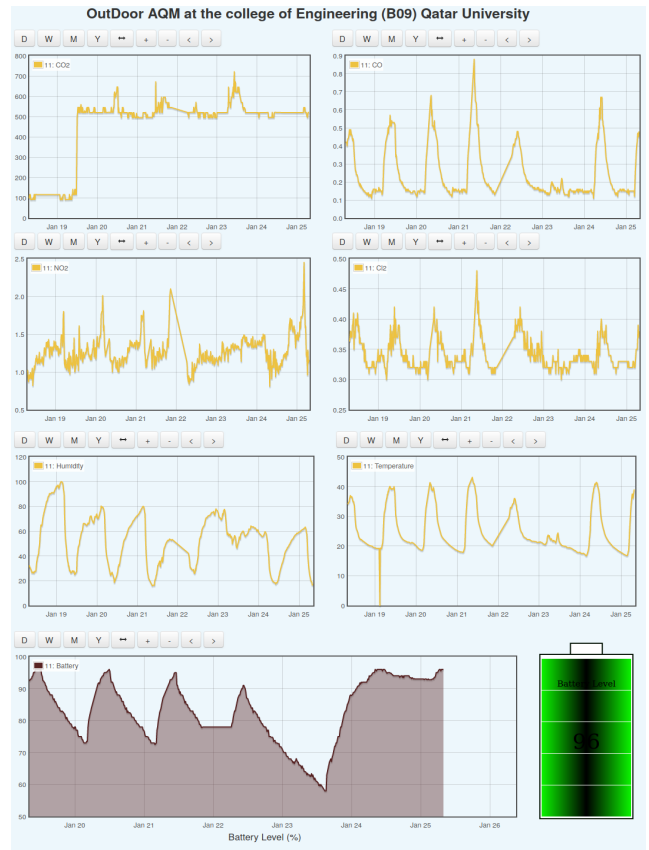


Fig. 6. Outdoor Air quality monitoring using solar panel as energy harvesting (B09 Qatar University : sub-urban site).

- [6] U. EPA, "Epa's report on the environment," Tech. rep., US Environmental Protection Agency (US EPA), Tech. Rep., 2008.
- [7] L. T. Padró-Martínez, A. P. Patton, J. B. Trull, W. Zamore, D. Brugge, and J. L. Durant, "Mobile monitoring of particle number concentration and other traffic-related air pollutants in a near-highway neighborhood over the course of a year," *Atmospheric Environment*, vol. 61, pp. 253–264, 2012.
- [8] D. V. Petrov, I. Matrosova, and A. Tikhomirov, "Raman gas analyzer applicability to monitoring of gaseous air pollution," in *21st International Symposium Atmospheric and Oceanic Optics: Atmospheric Physics*, vol. 9680. International Society for Optics and Photonics, 2015, p. 96803C.
- [9] M. Wang, T. Zhu, J. Zheng, R. Zhang, S. Zhang, X. Xie, Y. Han, and Y. Li, "Use of a mobile laboratory to evaluate changes in on-road air pollutants during the beijing 2008 summer olympics," *Ifolder Import 2019-10-08 Batch 8*, 2009.
- [10] F. Kizel, Y. Etzion, R. Shafran-Nathan, I. Levy, B. Fishbain, A. Bartonova, and D. M. Broday, "Node-to-node field calibration of wireless distributed air pollution sensor network," *Environmental Pollution*, vol. 233, pp. 900–909, 2018.